Proceedings of the 17th International Heat Transfer Conference, IHTC-17
14 – 18 August 2023, Cape Town, South Africa

IHTC-17 | ID: 119

MEASUREMENT OF TEMPERATURE EFFECTS ON VOID GENERATION IN ELECTROMIGRATION USING THERMO-REFLECTANCE IMAGING

K. Tatsumi[1*], K. Araki[1], K. Tamai[1], R. Kuriyama[1] and K. Nakabe[1]

[1]Kyoto University, Kyotodaiagku-katsura, Nishikyo-ku, Kyoto 615-8540, Japan

ABSTRACT

In electronic devices, a high-density electric current applied to the wires causes atoms or vacancies drifts, which is called electromigration. Electromigration produces voids and holes at the cathode side, especially at the wire ends and Via, eventually causing wire failure. The atom and void mass flux due to electromigration is affected by the current density, atom (or void) concentration, stress, and temperature. In this study, we investigated the effects of temperature and heat transfer on void generation, void growth, and microwire failures associated with electromigration. Thermo-reflectance imaging (TRI) was used to simultaneously measure the two-dimensional temperature distributions with the visualization of the voids. The TRI technique was validated by comparing the temperature distribution of an Au microwire heated by Joule heating to numerical computation results. Electromigration measurements were conducted using an Al microwire in which void generation was observed at the cathode end. The growth pattern of the void changed with time, giving different curves for the increasing rate of void size. Furthermore, the local temperature and its gradient significantly affected the void growth. The void growth rate and local temperature exhibited an exponential relationship, highlighting that the diffusivity of the atom (void) plays an important role in local void growth characteristics.

KEY WORDS: Electromigration, Micro-wire, Void, Joule heating, Temperature, Thermo-reflectance imaging

1. INTRODUCTION

Thermal damage is an important issue in semiconductors and electronic devices. Local temperature increase owing to Joule heating can become significant as the wire size of these devices are markedly reduced. The high-temperature condition induces thermal fatigue and failure at the wires and gates of the semiconductor and accelerates electromigration and stress migration, resulting in wire breakage (failure). Electromigration is a phenomenon wherein the metal wire atoms migrate and diffuse, and is driven by the electron collision of the electric current. The atom migration decreases the atom density on the cathode side and generates voids and holes in the wire. As electromigration progresses, void growth occurs, which eventually causes an open circuit to form [1,2]. Electromigration magnitude increases significantly with increasing current density and temperature. Therefore, reliability evaluation of lifetime failure due to electromigration is important for miniaturized wiring and interconnections in electronic devices, and numerous studies have been conducted to understand and model electromigration since the 1960s. From these studies, it is commonly understood that the atom (or vacancies) flux in electromigration relies on the current density, overall temperature, and physical properties of the wire material such as the diffusion coefficient [1-4].

With the advancement of electronic devices, a higher accuracy is required for modern device reliability analysis. To understand and model the reliability and lifetime of the wire accurately, the transient

*Corresponding Author: tatsumi@me.kyoto-u.ac.jp

characteristics of electromigration and effects of local physical quantities should be investigated in addition to the average and overall characteristics. As previously mentioned, the effects of current density, average temperature, and external factors on void generation and wire failure have been studied extensively [1-4]. However, the effect of the temperature distribution on void generation, growth, and coalescence is largely unknown, especially for the time characteristics, owing to measurement difficulties [5,6].

Herein, we visualized the time variation of void size and location, and simultaneously measured the surface temperature distribution of an Al microwire (electrode) when electric current was applied to induce electromigration. The thermoreflectance imaging (TRI) technique was used to measure the two-dimensional temperature distribution. The TRI method measures variations in the target surface reflectance by measuring the intensity of the pulsed light reflection after irradiation on the surface using a high-resolution camera. The camera measurement and sub-micron second light pulse realizes the two-dimensional measurement with high spatial and temporal resolutions. The resolution of the TRI method applied herein is on the order of submicron in space (~500 nm) and nanosecond in time (~200 ns). To validate the measurement method, the temperature distribution of a 10 μm wide Au wire under Joule heating was compared with numerical calculation results. The area of the void generated by electromigration was measured as a function of time at the cathode side of the Al wire, whose width and thickness were 10 μm and 75 nm, respectively. The distribution can be divided into three regions based on the slopes of the log-log graphs. These regions represent different void states, namely, the void appearance at the wire surface, increasing size of each void (void growth), and void coalescence. Furthermore, the effects of temperature and its gradient in the regions upstream, downstream, and between the voids on the void growth rates were evaluated.

2. EXPERIMENTAL METHODS

TRI measures the two-dimensional distribution of surface temperature by examining material reflectance changes with temperature (thermo-reflectance). The surface temperature is obtained by measuring the reflectance and applying the following relationship:

$$\Delta R = \frac{\partial R}{\partial T} \Delta T \tag{1}$$

Where R and T are the reflectance and temperature, respectively. With the reflected light intensity denoted as I, we obtain the relationship between the variation in I and T as follows:

$$\frac{\Delta I}{I} = \left(\frac{1}{R}\frac{\partial R}{\partial T}\right) \Delta T = C_{\mathrm{TR}} \Delta T \tag{2}$$

In Eq. (2), the relation enclosed in parentheses is the thermoreflectance coefficient C_{TR}. The value of C_{TR} is a physical property of the material and depends on the light wavelength. The TRI method irradiates the material with light of a specific wavelength and measures the reflectance, which can then be converted to temperature. Thermoreflectance measurements are generally used to determine the thermal conductivity of a material. In such measurements, laser is used as the light source to heat the material, and a photomultiplier is used as the light detector. For the TRI technique, a camera was used to measure the two-dimensional distribution of reflection [7]. Unlike point measurements, the two-dimensional distribution of the instantaneous (phase average) temperature can be obtained. However, the measurement accuracy decreases as the reference light cannot be obtained from the same light source, and the camera may exhibit a lower sensitivity than the photomultiplier. Furthermore, accurate position control in the planar and focal directions of the object during the measurement and post image processing are important for temperature measurement accuracy.

Fig. 1 shows a schematic of the measurement apparatus. An LED was used as the light source and the object was irradiated with light through a half mirror and an objective lens. Reflection images were recorded using

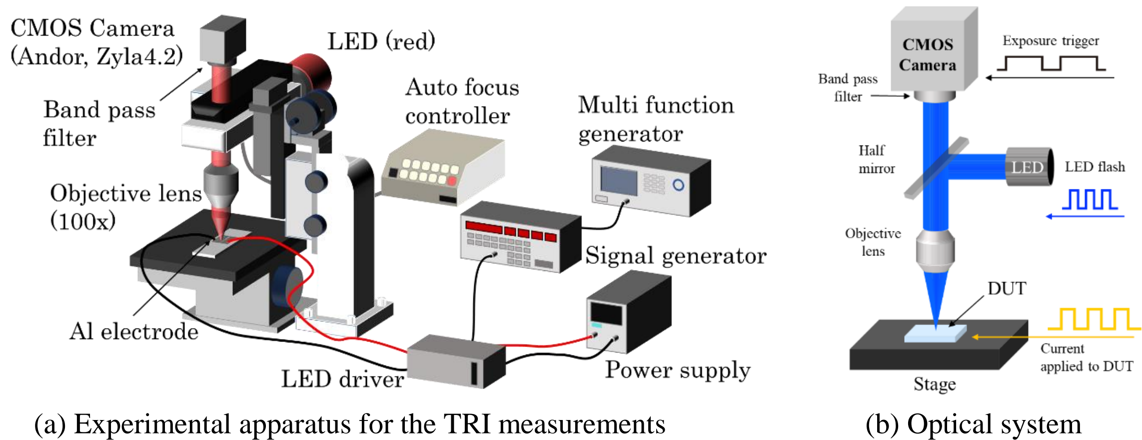

(a) Experimental apparatus for the TRI measurements (b) Optical system

Fig. 1 Schematic of the experimental apparatus and optical system for the TRI measurement.

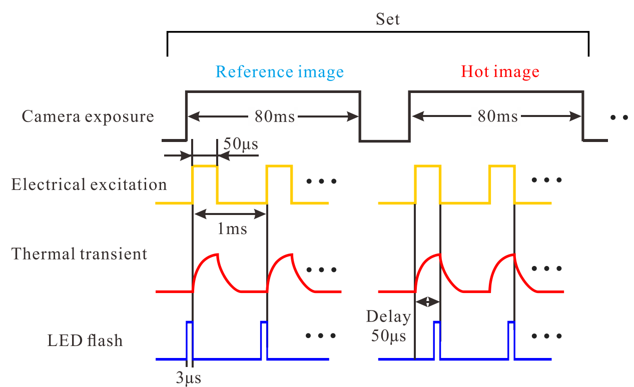

Fig. 2 Timing chart of camera exposure, current supply, and LED flash for the TRI measurement.

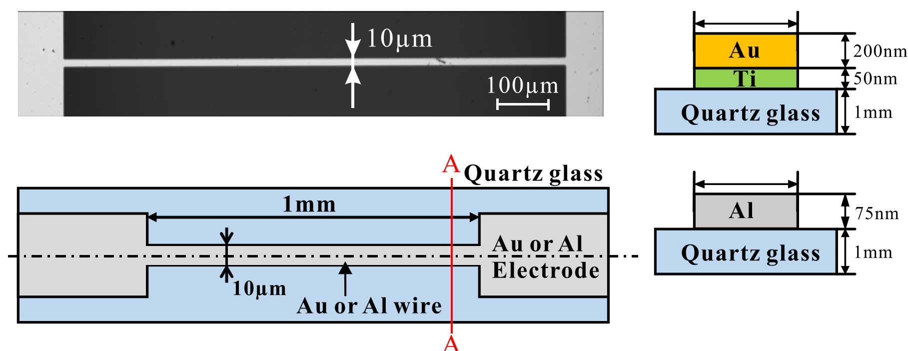

Fig. 3 Photograph and schematic of the Au and Al micro-wires.

a CMOS camera (Andor, Zyla 4.2 plus). An autofocus system was installed in the measurement system to obtain focused images during the measurement.

For wires of electronic devices that suffer from electromigration, the applied electric current varies periodically and irregularly over time. Therefore, we periodically applied current to the microwire, which will be shown shortly, in a square waveform. This process also increases the measurement accuracy because a thermal steady state is difficult to obtain using Joule heating devices. In addition, periodic heating can reduce the effect of object drift caused by thermal expansion. Fig. 2 shows the timing chart of the applied measurements. The signal for the camera exposure, current supplied to the wire, and LED flash were

synchronized. The camera exposure time was set to 80 ms and several cycles of current supply (heating) were applied during one camera exposure with an LED flash emitted at a specific phase during each current supply. The time widths of the current supply and LED flash were 50 and 3 μs, respectively. The period of these cycles was 1 ms, and the number of cycles in each exposure was 55. Several flash cycles applied during exposure can increase the reflection image intensity. The LED flash was emitted under two timing conditions in each cycle: one immediately before the current was applied and the other before the current supply ended. The former timing provides images of the object under cooled conditions (reference image) and that obtained by the later timing gives the maximum temperature (hot image). The reference and hot images were taken alternately as a set, and 10,000 sets were measured for each measurement.

Fig. 3 shows the Au and Al wires used for the measurements, where the Au wire was used to validate the measurement method. The width, length, and thickness of the Au wires were 10 μm, 1 mm, and 200 nm, respectively. The Al wires were used for the electromigration experiments with widths, lengths, and thicknesses of 10 μm, 1 mm, and 75 nm, respectively. The Au and Al wires were patterned on quartz glass using electron beam deposition and lithography. For the Au wire, a 50 nm thick Ti layer was deposited between the Au and glass as a bonding layer.

3. RESULTS AND DISCUSSION

3.1 Calibration Measurements The thermo-reflectance coefficient C_{TR} was obtained from the relationship between temperature and reflectance. Calibration was conducted using a constant-temperature stage and thin films of Au and Al. A 200 nm thick film was patterned on quartz glass and placed on the stage and the film reflectance was measured at various temperatures. The surface temperature was measured using a thermocouple attached to the surfaces of the Au and Al films. Blue (center wavelength 470 nm) and orange LEDs (center wavelength 617 nm) were used for the Au and Al measurements, respectively, and were chosen to maximize the C_{TR} values [8, 9]. The objective lens magnification was x100 (Olympus, LMPLFLN NA=0.8) and the image resolution was 65 nm/pixel.

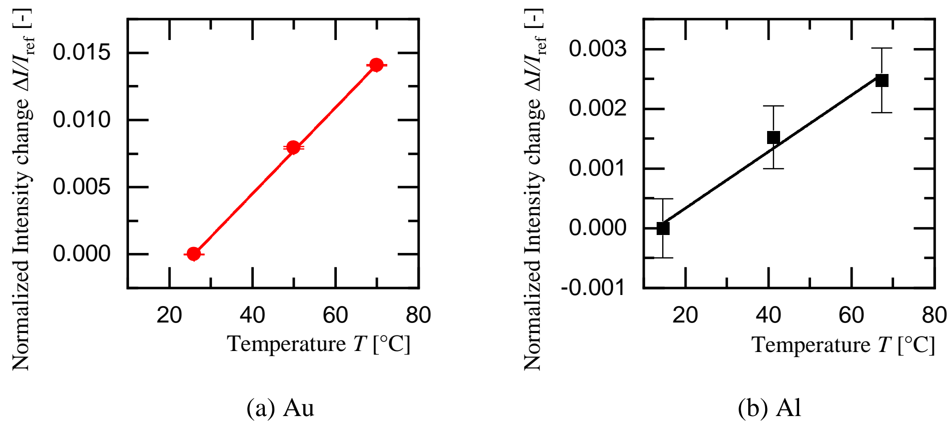

Fig. 4 Calibration measurement of the thermo-reflectance coefficient C_{TR} using Au and Al films deposited on glass substrates.

The relationship between the film temperature and normalized intensity $\Delta I/I_{ref}$ is shown in Fig. 4 and the data for Au show a positive slope (Fig. 4(a)). The C_{TR} value obtained from the graph was 3.20×10^{-4} K^{-1}, which agrees well with the sign and value of 3.40×10^{-4} K^{-1} reported by Tesseir et al. [8] and Fabaloro et al. [9]. Although not shown here, the C_{TR} measured using a green LED light showed a negative value, which agrees with the reports by Tesseir et al. [8] and Kendig et al. [10]. The C_{TR} value obtained for the Al wire is shown in Fig. 4 (b) at 1.54×10^{-4} K^{-1}, in good agreement with the value of 1.4×10^{-4} K^{-1} reported by Fabaloro et al. [9].

3.2 Validation To validate the two-dimensional temperature measurements, we applied an electric current to the Au wire, as shown in Fig. 3(a), and measured the temperature distribution caused by Joule heating using the TRI method. The experimentally obtained results were compared with those of a numerical simulation. A current of 100 mA was applied to the wire with a period of 200 μs and a 5% duty rate (current-applied time of 10 μs). The measurement timing was 9 μs after the current was applied, which captured the highest temperature moment. Fig. 5(a) shows the measured temperature distributions of the wire and connecting electrodes, while Fig. 5(b) shows the temperature distribution along the wire centerline from the connecting electrode to a certain point on the wire indicated by the dashed line in Fig. 5(a).

In Fig. 5(a), a temperature increase is observed at the wire, which was attributed to Joule heating. The temperature decreases significantly at the ends of the wire owing to heat conduction to the connecting electrodes. Numerical computations were conducted using the COMSOL Multiphysics software (ver. 4.3) to solve the heat conduction equation for the domain, which includes the Au wire, connecting electrode, and glass substrate. The calculation results are shown as solid lines in Fig. 5(b). The temperature distributions of the computation and experimental measurements agreed well, confirming the validity of the measurements.

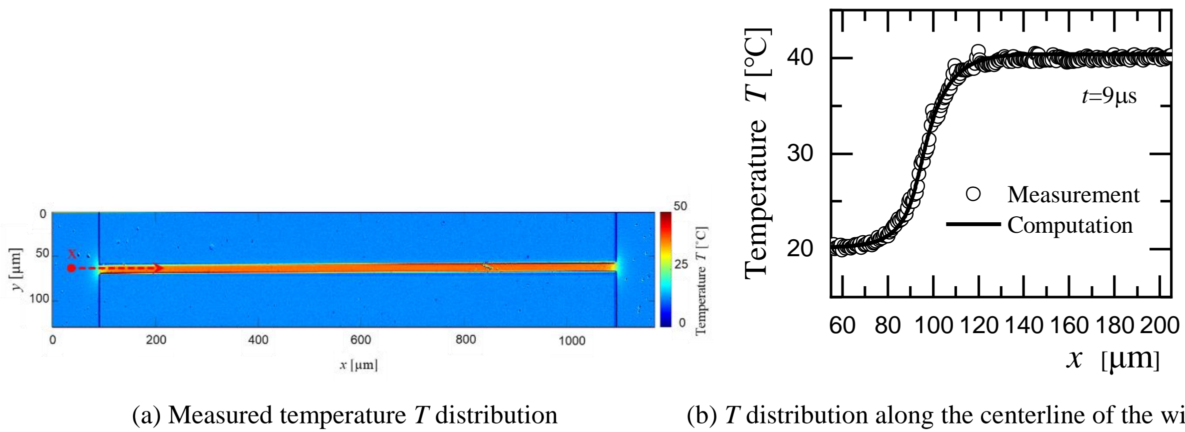

(a) Measured temperature T distribution (b) T distribution along the centerline of the wire

Fig. 5 Temperature measurement of Au wire under Joule heating and comparison with numerical computation of the temperature along the centerline near the longitudinal ends of the wire.

3.3 Electromigration in the Al wire Measurement of the effects of electromigration and temperature on void generation was conducted using an Al wire. An electric current of 32 mA was supplied to the wire to apply a current density 4.4×10^6 A/cm^2.

Fig. 6 shows the results of the bright-field observations and temperature distribution measured by the TRI method at the cathode side. The value t is the elapsed time after the voltage was applied to the Al wire. Fig. 6(a) and (e) show the results before applying current to the wire. Fig. 6(b) and (f) are for t=945 s, and Fig. 6(c) and (g) are for t=1062 s, respectively. Fig. 6(d) shows a photograph of the Al wire after wire breakage (failure) at t=1071s, and Fig. 6(h) shows a magnified view of Fig. 6(d).

As shown in Fig. 6 (a)–(d), void (hole) generation in the Al wire and their growth until wire breakage (failure) can be clearly visualized. During the initial stage of void generation, voids appear at the surface and increase in size. The void size fluctuated as it grew and even decreased at some points (void filling), but not observed again once the void reached a certain size. Subsequently, the voids began to coalesce as they reached a critical size and number. Void coalescence developed into voids connections in the spanwise direction, and the wire failed when the void connection extended across the wire width. Considering that the current density of the Al wire was 4.4×10^6 A/cm^2, the main cause of void generation and growth was the transport of Al atoms driven by electromigration. In addition, the low aspect ratio of the

Al wire can produce a certain amount of stress migration caused by the internal stress gradient formed in the wire [3].

Fig. 6(e)–(g) show the local temperature increases in the Al wire with increasing void size. The wire temperature was approximately 35 °C at t=0 s, which was used to determine the overall temperature increase at the moment the current was supplied. At t=945 and 1062 s, the overall temperature of the wire increased to approximately 45 °C, and a significant high-temperature region appeared near the end of the wire. This was attributed to the increase in local current density and local heat flux caused by void generation, which decreased the cross-sectional area of the wire.

Comparing the void pattern and temperature distributions shown in Fig. 6(c), (d), and (g), the temperature in the x=22–27 μm area was 55 °C, and a large temperature gradient developed near this region. Comparing Fig. 6(c) and (d), the area at which the wire fails corresponds to the high-temperature regions; and to be more precise, the region of large temperature gradients. The migration (drift) velocity of the Al atoms (or vacancies) due to electromigration is proportional to the diffusivity, current density, atom (vacancy) concentration, and stress [2]. Temperature affects the diffusivity and atom (vacancy) mobility, and the migration velocity varies in regions with a large temperature gradient. In these regions, the atom (vacancy) concentration increases or decreases, depending on the temperature gradient sign. In the previously shown results, wire failure was observed where a positive temperature gradient existed. The difference in the local migration velocity owing to the temperature gradients enhanced void generation and led to wire failure. This trend agrees well with theoretical analysis, which has long been discussed in electromigration research. Herein, we were able to visualize this phenomenon locally and continuously over time.

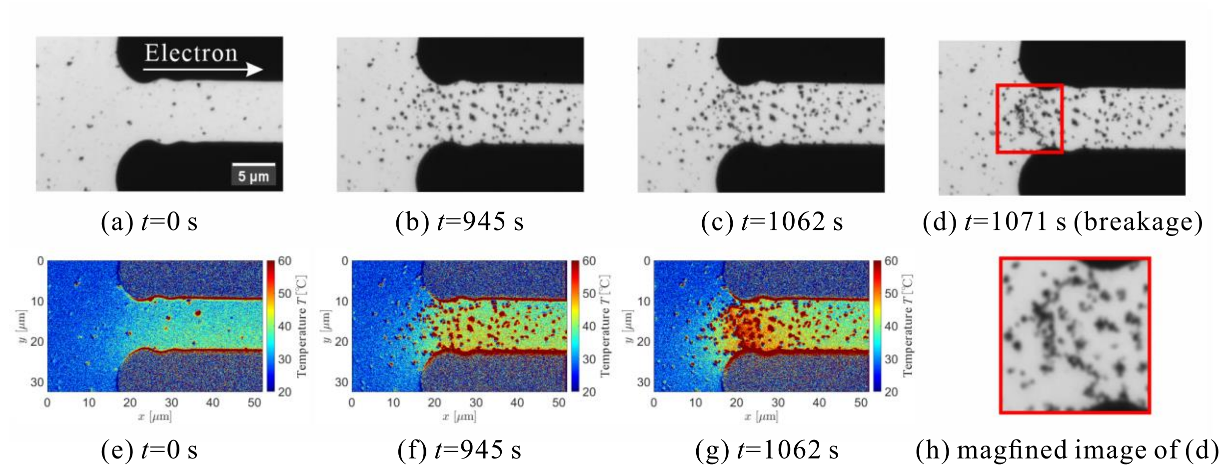

Fig. 6 Photographs and temperature distribution of the Al wire at the cathode side with electromigration effects. (a)–(d) Bright field views of the wire; (e)–(g) TRI measurements; (h) Magnified view of the area shown by the red square box in (d).

To evaluate the characteristics of void generation and growth, the void areas in the images were measured. Fig. 7(a) shows the sum of the void area sizes A_v and the local temperature of the wire T in relation to the current supply time t on a log-log graph. The temperature was measured at a point close to the area where the wire broke. The vertical axes of the areas A_v and T are shown on the left and right sides of the graph, respectively.

In Fig. 7(a), A_v increases with time, showing three regions with different slopes of the power law at t=0–3000, 3000–5650, and 5650–8864 s, denoted as Phases 1, 2, and 3, respectively. Phase 1 is the period wherein the void nucleus generates in the Al wire and begins to appear at the wire surface as it increases in size [2]. During Phase 2, the voids observed at the surface expanded. And Phase 3 featured void coalescence with the connection extending in the spanwise direction. In this case, the area of the current

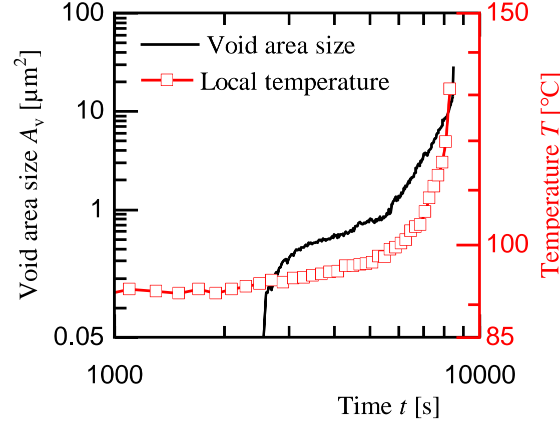

Fig. 7 Time profile of the void area size (total) and local temperature at a position near the wire breakage area.

path (non-void area) of the wire decreased significantly following the phenomena similar to percolation theory. Therefore, A_v and T significantly increased during this phase.

To discuss the effect of the base temperature on void generation and wire failure characteristics, the void growth rate was compared between two base temperature conditions. That is, the glass substrate was set at room temperature and high temperature by placing the substrate on a hot plate at 112 °C. The area of each void appearing on the wire surface was measured together with the local temperature near each void. The void growth rate was then evaluated using the rate of increase of the number of vacancies per unit time $\Delta N/\Delta t$ as shown in Eq. (3):

$$\frac{\Delta N}{\Delta t} = N_v d \frac{\Delta A_v}{\Delta t} \tag{3}$$

Where N is the number of vacancies, N_v is the number of vacancies per volume, d is the Al wire thickness, and A_v is the void area. The average values of $\Delta N/\Delta t$ for the room and high-temperature conditions were 1.28×10^6 and 5.17×10^6 s^{-1}, respectively. We then applied the following equation for curve fitting to the data (n=21) obtained from the base temperature of high-temperature.

$$\frac{\Delta N}{\Delta t} = \exp(aT + b) \tag{4}$$

Parameters a and b were $a=1.97\times10^{-2}$ K^{-1} and b=12.35, respectively. We then extended the function to the low-temperature region. The deviation of the data obtained at the base temperature of room temperature from the function was evaluated and the value was 13%. Therefore, the relationship between the void growth rate and local temperature follows an exponential function. This is reasonable because the temperature effect on the migration velocity of the atom (vacancy) mainly appears in the diffusivity. The temperature and diffusivity have an exponential relationship, and that is what was reflected in the experimental results based on the local temperature and void growth characteristics.

4. CONCLUSIONS

Visualization of void generation and growth due to electromigration and temperature measurement using thermo-reflectance imaging was achieved for Al microwires after electric current application. Void generation was observed on the cathode side of the Al wire. Based on the visualization of the void and

the total void area, the void generation process could be divided into three phases. Voids appeared discretely on the wire surface, increase in size, and finally coalesce, which can be clearly observed in the relationship between the void size and time. The temperature measurements showed that Joule heating increased the overall wire temperature and the local temperature at which the voids were generated. The voids decreased the cross-sectional area of the wire, which increased the current density and heat flux, leading to a large temperature gradient. The high temperature and large gradient enhanced the void migration velocity owing to the increased diffusivity. The effect of temperature on the void generation characteristics was accurately fitted using an exponential function.

ACKNOWLEDGMENT

This work was partially supported by the Japan Society for the Promotion of Science KAKENHI Grant Number 21H01262 and by the Kyoto University Nanotechnology Hub in "Advanced Research Infrastructure for Materials and Nanotechnology Project" sponsored by the Ministry of Education, Culture, Sports, Science and Technology (MEXT), Japan.

REFERENCES

[1] Ho, P. S. and Kwok. T., "Electromigration in metals," *Reports on Progress in Physics*, 52, pp. 301-348, (1989).

[2] Rosenberg, R. and Ohring, M., "Void Formation and Growth During Electromigration in Thin Films," *Journal of Applied Physics*, 42, pp. 5671-5679, (1971).

[3] McPherson, J. W. and Dunn, C. F., "A Model for Stress-Induced Metal Notching and Voiding in Very Large-Scale-Integrated Al-Si(1%) Metallization," *Journal of Vacuum Science and Technology*, B5, 42, pp. 1321-1325, (1987).

[4] Hu, C.-K., "Electromigration Failure Mechanism in Bamboo-Grained Al (Cu) Interconnections," *Thin Solid Films*, 260, pp. 124-134, (1995).

[5] Tian, H., Ahn, W., Maize, K., Si, M., Ye, P., Alam, M. A., Shakouri, A., and Bermel, P., "Thermoreflectance Imaging of Electromigration Evolution in Asymmetric Aluminum Constrictions," *Journal of Applied Physics*, 123, pp. 035107, (2018).

[6] Wang, Z., Alajlouni, S., Bermel, P., and Shakouri, A., "Explaining an Unusual Electromigration Behavior—A Comprehensive Experimental and Theoretical Analysis Using Finite Element Method," *Journal of Applied Physics*, 129, pp. 214502, (2021).

[7] Farzaneh, M. Maize, K., Lüerßen, D., Summers, J. A., Mayer, P. M., Raad, P. E., Pipe, K. P., Shakouri, A., Ram, R. J., and Hudgings, J. A., "CCD-based Thermoreflectance Microscopy: Principles and Applications," *Journal of Physics D: Applied Physics*, 42 (14), pp. 143001, (2009).

[8] Tesseir, G. Hole, S., and Fournier, D., "Quantitative Thermal Imaging by Synchronous Thermoreflectance with Optimized Illumination Wavelengths," *Applied Physics Letters*, 78 (16), pp. 2267-2269, (2001).

[9] Favaloro, T., Bahk, J.-H. and Shakouri, A., "Characterization of the Temperature Dependence of the Thermoreflectance Coefficient for Conductive Thin Films", *Review of Scientific Instruments*, 86 (2), pp. 024903, (2015).

[10] Kendig, D., Yazawa, K., and Shakouri, A., "Hyperspectral Thermoreflectance Imaging for Power Devices", *33rd Thermal Measurement, Modeling & Management Symposium*, pp. 204-207, (2017).